Radiochemical Studies of the Fission of U^{235} Induced by Helium Ions*

R. GUNNINK† AND J. W. COBBLE
Department of Chemistry, Purdue University, Lafayette, Indiana
(Received March 9, 1959)

The absolute fission yields of approximately twenty-five nuclides from the helium-ion-induced fission of U^{235} were determined with an accuracy of ±5–15% for several energies ranging from 20 to 40 Mev. Such features of fission as the symmetric-asymmetric modes of fission, the relation of total fission cross section to compound nucleus theory, fine structure in fission product distribution, valley to peak ratios, and neutron emission are discussed as well as some of the experimental detail involved.

INTRODUCTION

RADIOCHEMICAL studies have played an important role in the detailed characterization of the phenomenon of fission. Much of the early work was concerned with low-energy fission (i.e., thermal neutron fission) and although a considerable amount of work is still being done in this area, efforts have recently been directed toward a study of fission induced by higher-energy particles.

Among the first studies made with high-energy particles are those of Goeckermann and Perlman[1] using 190-Mev deuterons to induce fission in Bi^{209} and by Batzel, Seaborg, and Miller[2,3] who used 340-Mev protons, 190-Mev deuterons, and 190- and 380-Mev helium ions to induce fission in copper and other medium-weight elements. Later, bombardments were made using ions of intermediate energy (<50 Mev). Newton[4] studied the fission of thorium with helium ions and Tewes and James[5,6] produced fission in the same element using protons. A review of the early work done at high energies has been given by Spence and Ford.[7] Seaborg and co-workers have obtained some preliminary information on fission in a series of investigations primarily aimed at a study of spallation-fission competition.[8–11] These include data on the fission of U^{233}, U^{235}, U^{238}, Np^{237}, and Pu^{239}.

Other studies at intermediate[12] and high energies[13–15] have been made and recently work involving fission induced by 20- to 200-Mev protons and deuterons[16] and 5- to 14-Mev neutrons[17,18] has appeared.

The work of Seaborg and co-workers showed one unexpected feature: the onset of symmetric fission at excitation energies for some nuclides as low as 30–40 Mev. The previous data would not have indicated this trend for these nuclides. Unfortunately, most of the fission yield work at higher energies was not done with sufficient accuracy to delineate any but the gross features of the fission yield curve. This has been partly due to insufficient decay scheme information on some fission product nuclides and also because only the gross effects of fission were being studied. However, with improved decay data and more advanced instrumentation and chemical methods, it should be possible to examine more of the details of fission, to resolve the question as to the onset of symmetric fission, and to determine nuclear radii from the resulting total fission and previously available spallation cross sections.

In the first of a series of investigations in this laboratory, attention was focused on the fission cross sections of U^{235} induced by 20- to 40-Mev helium ions. To obtain the desired accuracy more rigorous and precise experimental procedures were developed.

EXPERIMENTAL PROCEDURE

A. Target Preparation

The uranium targets were prepared by the electrodeposition method described by Hufford and Scott.[19] The plating solution consisted of 100 microliters of 0.2*M* enriched (93.41%) uranium-235 nitrate solution, 2 ml of 0.4*M* $(NH_4)_2C_2O_4$, and 0.5 ml of H_2O. The solution was adjusted to a *p*H of 5 with NH_4OH, and then heated to about 70–80°C. Plating was started initially at a low current density and was then rapidly increased to about 200–250 ma/cm². From 3–5 minutes were

* This research was supported by the U. S. Atomic Energy Commission; from the Ph.D. thesis of R. Gunnink, June 1959.
† Procter and Gamble Fellow, 1957–58.
[1] R. H. Goeckermann and I. Perlman, Phys. Rev. **76**, 628 (1949).
[2] Batzel, Miller, and Seaborg, Phys. Rev. **84**, 671 (1954).
[3] R. E. Batzel and G. T. Seaborg, Phys. Rev. **82**, 607 (1951).
[4] A. S. Newton, Phys. Rev. **75**, 17 (1949).
[5] H. S. Tewes and R. A. James, Phys. Rev. **88**, 860 (1952).
[6] H. A. Tewes, Phys. Rev. **98**, 25 (1955).
[7] R. W. Spence and G. P. Ford, *Annual Review of Nuclear Science* (Annual Reviews, Inc., Palo Alto, 1953), Vol. 2, p. 399.
[8] Glass, Carr, Cobble, and Seaborg, Phys. Rev. **104**, 454 (1956).
[9] S. E. Ritsema, M.S. thesis, University of California Radiation Laboratory Report UCRL-3266, 1956 (unpublished).
[10] Vandenbosch, Thomas, Vandenbosch, Glass, and Seaborg, Phys. Rev. **111**, 1358 (1958).
[11] W. M. Gibson, Ph.D. thesis, University of California Radiation Laboratory Report UCRL-3493, 1956 (unpublished).
[12] R. W. Spence, Atomic Energy Commission Report AECD-2625, June, 1949 (unpublished).
[13] Hicks, Stevenson, Gilbert, and Hutchin, Phys. Rev. **100**, 1284 (1956).
[14] W. E. Nervik and G. T. Seaborg, Phys. Rev. **97**, 1092 (1955).
[15] Folger, Stevenson, and Seaborg, Phys. Rev. **98**, 107 (1955).
[16] Stevenson, Hicks, Nervik, and Nathaway, Phys. Rev. **111**, 886 (1958).
[17] Sugihara, Drevinsky, Troianello, and Alexander, Phys. Rev. **108**, 1264 (1958).
[18] J. G. Cuninghame, J. Inorg. and Nuclear Chem. **5**, 1 (1957).
[19] D. L. Hufford and B. F. Scott, *The Transuranium Elements: Research Papers* (McGraw-Hill Book Company, Inc., New York, 1951), National Nuclear Energy Series, Plutonium Project Record, Vol. 14B, Div. IV, p. 1149.

required to deposit ~300 mg/cm² of uranium onto an aluminum disk in a circular area of ~1.4 cm².

The uranium targets so prepared were assayed by alpha counting in a 2π windowless proportional counter. The observed disintegration rate was converted to mg/cm² using the appropriate specific activity (the U^{235} analysis was made by mass spectrometry), and by using the self-absorption and backscattering corrections determined by others.[20,21] Each target was also "sectored" by systematically counting the target when covered in various positions with a plate containing a small hole. Targets whose nonuniformity was greater than ±2% were discarded.

The target area was determined by taking an average of several measurements of the diameter of the area plated. The value thus obtained is believed to have an accuracy of about 1 to 2%.

B. Target Assembly and Bombardments

Bombardments were made with the Argonne National Laboratory Cyclotron. The range of the helium ion beam was 189 mg/cm² of aluminum. Absorbers made from 2-*S* aluminum were used to degrade the beam to the desired energy. Range-energy relationships for protons have recently been determined for several materials.[22] Since these relationships were experimentally determined, it is believed that they are more reliable than the older range-energy curves obtained by theoretical considerations by Aron, Hoffman, and Williams.[23] The discrepancy is quite large, resulting in a difference of nearly 1 Mev for 40-Mev helium ions. Small corrections due to the thermal expansion of aluminum when heated by the beam were also made resulting in a 1% lower absorber surface density.

Since a high neutron flux is created by (α,xn) reactions on the aluminum degrading foils and environment, the neutron-induced "background" fission yield was determined by placing a target behind thick absorbers in the target assembly where $E \leqslant 15$ Mev. The neutron-induced cross section was found to be comparable to the true helium-ion-induced cross section at a beam energy of ~20 Mev under the experimental conditions used, and was subtracted from all runs where it was significant.

C. Chemistry Separation Procedures

A known amount (5–10 mg) of carrier elements in various but common oxidation states corresponding to each radioisotope to be used to determine the isobaric fission mass yield was combined to form a solution in which the irradiated target was dissolved. The chemical scheme devised for the separation and purification of all of the radioelements is given in the Appendix.

D. Counting Procedures

From the previous literature it was apparent that probably one of the largest errors in the determination of fission cross sections is introduced by inaccurate counting. To reduce this source of error, counting corrections were experimentally determined for a large number of the fission product nuclides for counting in a 2π window proportional flow counter. For these nuclides, the self-absorption and self-scattering factors, the geometry factors, and the backscattering coefficients have been determined by previously standardizing the isotope involved by 4π[24–27] and by $4\pi\ \beta-\gamma$[28,29] coincidence counting methods. These counting corrections are the subject of another communication.[30] It is believed that a major portion of the errors introduced by using semi-empirical factors in converting the observed counting rate to the absolute disintegration rate have been eliminated and the remaining errors involved in the procedure should not in general be greater than 3–5%.

A 5-in. well-type NaI(Tl) crystal has also been calibrated[31] for photopeak counting efficiency and was used for the yield determinations of Ru^{103}, Ru^{105}, I^{131}, I^{133}, Ce^{141}, and Ce^{143} since it was found considerably easier to count these isotopes by this means. For these isotopes, the errors so involved are somewhat less than for proportional beta counting.

E. Treatment of the Counting Data

Several key isotopes in the fission yield curve are complicated by their decay schemes and isotopic mixtures. One of the most complicated resolutions involves the isotopes Sr^{89}, Sr^{91}, Sr^{92}, Y^{91}, and Y^{92}. In this particular case, the mass yields for masses 89 and 91 are obtained quite accurately but that of mass 92 cannot be determined as accurately because of resolution difficulties.

The I^{131} determination is complicated by the fact that one does not know in what ratio its Te^{131m} and Te^{131} parents are populated in primary fission events. The following procedure was used to estimate how these states are populated:

(1) The shell model of the nucleus regarding spin states was assumed[32] to apply. (See Fig. 1.)

[20] Cunningham, Ghiorso, and Jaffey, see reference 19, p. 1198.
[21] A. H. Jaffey, *The Actinide Elements* (McGraw-Hill Book Company, Inc., New York, 1954), National Nuclear Energy Series, Plutonium Project Record, Vol. 14A, Div. IV, p. 596.
[22] Bichsel, Mozley, and Aron, Phys. Rev. **105**, 1788 (1957).
[23] Aron, Hoffman, and Williams, Atomic Energy Commission Report AECU-663, May, 1951 (unpublished).
[24] B. D. Pate and L. Yaffe, Can. J. Chem. **33**, 15, 610, 929, 1656 (1955).
[25] H. H. Seliger and L. Cavallo, J. Research Natl. Bur. Standards **47**, 41 (1951).
[26] H. H. Seliger and W. B. Mann, J. Research Natl. Bur. Standards **50**, 197 (1953).
[27] H. H. Seliger and A. Schwebel, Nucleonics **12**, 54 (1954).
[28] R. Gunnink, L. J. Colby, Jr., and J. W. Cobble, Anal. Chem. **31**, 796 (1959).
[29] P. J. Campion, J. Appl. Radiation and Isotopes **4**, 232 (1959).
[30] R. Gunnink and J. W. Cobble (to be published).
[31] L. J. Colby, Jr., and J. W. Cobble, Anal. Chem. **31**, 798 (1959).
[32] E. Feenberg, *Shell Theory of the Nucleus* (Princeton University Press, Princeton, New Jersey, 1955), p. 23.

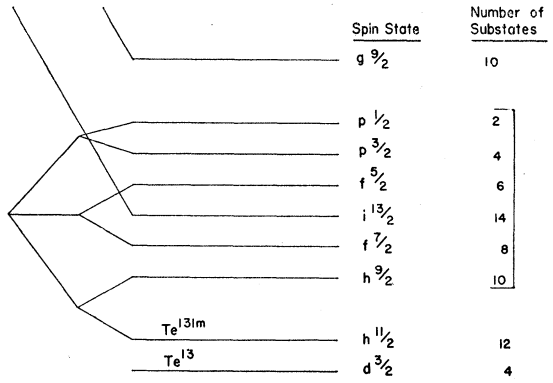

FIG. 1. Level diagram for Te^{131m}.

(2) From energy considerations, it was further assumed that the spin states bracketed in Fig. 1 will be the states populated.

(3) Nuclei in the 9/2 and 13/2 configurations were assumed to decay to the $h_{11/2}$ state; those in the $\frac{1}{2}$, $\frac{3}{2}$, and $\frac{5}{2}$ state decay to the $d_{3/2}$ level; and those in the $\frac{7}{2}$ level were assumed to decay with equal probability to both levels.

(4) The assumption that every substate would be populated with equal likelihood was also made, from which one can deduce that the percentage population for the $h_{11/2}$ and $d_{3/2}$ states of Te would be 63.5% and 36.5%, respectively.

(5) Sb^{131} was found by others[33] to decay to the ground state of Te^{131} 95% of the time. By using this procedure and the primary yield distribution curve the yield of mass 131 was determined.

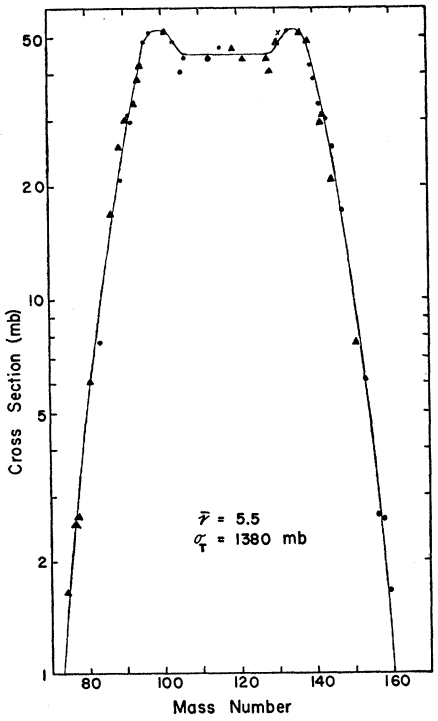

FIG. 2. Fission mass yield curve for 39.9-Mev helium ions. ▲ Reflection points; $\bar{\nu}$ average number of emitted neutrons.

[33] L. Glendenin (private communication).

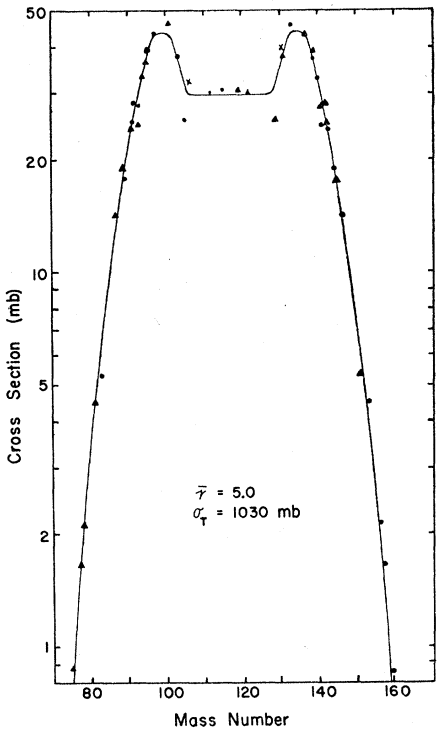

FIG. 3. Fission mass yield curve for 33.8-Mev helium ions. ▲ Reflection points; $\bar{\nu}$ average number of emitted neutrons.

Because, in fission, 25-min Se^{83m} is the parent of 2.3-hr Br^{83} only about 45% of the time,[34] the onset of the Br^{83} decay is effectively retarded and must be considered in the calculation of the isobaric yield of mass 83.

Two "milking" procedures were performed; Zn^{72}-Ga^{72} and Pd^{112}-Ag^{112}. In these cases Ga^{72} and Ag^{112} were separated from the parent isotopes and counted. The appropriate corrections were then made involving counting efficiencies, chemical yields, and time of initial and final separations. The method used to determine the independent yield corrections will be discussed in a later section.

EXPERIMENTAL RESULTS

Several duplicate bombardments were made at each energy, partially because of occasional losses of certain isotopes in the chemistry separation and partially to insure the accuracy of the data. When several duplicate isotopic yields were obtained, the "best value," which in most cases was the average value, was used as the uncorrected cross section for that isobaric yield. After the independent yields are added to that of the observed yield, the corrected isobaric cross section is

[34] J. M. Alexander and C. D. Coryell, Phys. Rev. **108**, 1274 (1958).

TABLE I. Fission cross sections (mb) for helium-ion-induced reactions of U^{235}. Each left-hand column lists the observed yield for each isotope. Each right-hand column lists the corrected cross section for the mass chain.

Energy (Mev)	39.9		33.8		28.2	
Isotope	σ[a]	σ_{corr}[b]	σ	σ_{corr}	σ	σ_{corr}
Zn^{72}	(0.43)	(0.43)	(0.085)	(0.085)		
Br^{83}	7.6	7.7	5.3	5.3	3.12	3.12
Sr^{89}	20.6 ±0.1(2)[c]	20.8	17.6 ±1.4(3)	17.7	11.3 ±0.7(2)	11.3
Sr^{91}	29.9 ±1.1(3)	31.0	24.7 ±0.3(3)	25.1	14.7 ±0.3(2)	15.0
Sr^{92}	28.0 ±1.5(2)	29.5	26.9 ±0.8(2)	28.2	15.6 ±2.0(2)	16.4
Y^{93}	(50)	(50)	27.6	27.9		
Zr^{95}	48.0 ±2.6(4)	48.6	39.0 ±0.8(4)	39.3	25.0 ±1.0(4)	25.1
Zr^{97}	49.0 ±1.2(4)	51.5	41.0 ±2.3(4)	43.0	26.5 ±1.7(4)	27.8
Ru^{103}	48.5 ±0.6(2)	48.5	37.7	37.7	22.5	22.5
Ru^{105}	39.8 ±1.8(2)	40.5	25.0	25.5	17.8	18.0
Ru^{106}	42.6 ±2.2(2)	44.0	(31)	(32)		
Pd^{112}	40.8 ±2.3(4)	43.3	28.8 ±2.2(3)	30.2	11.4 ±2.6	11.6
Cd^{115}	41.0 ±0.6(3)	46.7	27.6 ±1.6(2)	30.5	11.4	12.6
Cd^{115m}	5.0 ±0.15(2)		—			
I^{131}	33.0 ±1.6(2)	51.0	25.6 ±1.4(2)	39.7	16.7 ±0.4(2)	26.0
I^{133}	23.9 ±1.6(2)	52.0	23.7 ±0.7(2)	46.0	18.4 ±0.7(2)	32.3
Ba^{139}	31.2	42.2	28.5	37.0	17.0	22.0
Ba^{140}	22.0 ±0.2(3)	39.0	20.5/±0.7(3)	33.0	13.5 ±0.5(3)	21.0
Ce^{141}	32.0 ±0.9(3)	33.4	24.0 ±1.0(2)	24.7	17.5 ±0.7(3)	18.0
Ce^{143}	27.0 ±0.8(3)	30.3	22.0 ±1.3(4)	24.4	15.5 ±0.5(3)	17.0
Pr^{145}	23.4	25.8	17.5	19.0		
Nd^{147}	15.8 ±0.6(3)	17.2	13.4 ±0.8(3)	14.3	8.2 ±0.5(3)	8.7
Sm^{153}	5.2 ±0.14(3)	6.1	4.0 ±0.06(3)	4.5	2.7 ±0.4(3)	3.0
Eu^{156}	2.1 ±0.15(2)	2.65	1.54±0.14(2)	2.13	0.74	0.86
Eu^{157}	1.66±0.06(2)	2.55	1.16±0.12(2)	1.66	0.39	0.52
Gd^{159}	1.05±0.00(2)	1.67	0.68±0.03(2)	0.88	0.29	0.36
Tb^{161}	0.50	0.63			0.09	0.11
La^{140}[d]	8.1 ±0.7(2)		5.7 ±0.1(3)		2.2 ±0.15(2)	

Energy (Mev)	25.95		23.1[f]		20.5[g]		Neutron
Isotope	σ	σ_{corr}[e]	σ	σ_{corr}[e]	σ	σ_{corr}[e]	σ_{neut}
Br^{83}			0.66	0.62			
Sr^{89}	5.9	5.8	2.12±0.03(2)	2.00	0.38±0.02(2)	0.28	(0.16)
Sr^{91}	7.8	7.7	3.09±0.08(3)	2.95	0.57±0.09(2)	0.37	(0.20)
Sr^{92}	10.0	10.2	3.09±0.20(2)	3.07	(0.47)		
Zr^{95}			5.0 ±0.15(4)	4.7	0.56	0.37	(0.27)
Zr^{97}	15.3	15.2	5.0 ±0.19(4)	4.9	0.83±0.03(2)	0.56	0.28
Ru^{103}			3.15	2.97			
Ru^{105}			2.0	1.91	(0.104)		(0.055)
Ru^{106}			(2.0)	(1.94)			
Pd^{112}	5.9 0.1(2)	5.9					
Cd^{115}	4.63	5.0	1.10				
Cd^{115m}	...						
I^{131}			2.56	2.56	0.47	0.45	
I^{133}			3.5 ±0.3(2)	5.07	0.72	0.79	0.11
Ba^{139}	(9.07)	(10.5)					
Ba^{140}	8.70	11.5	3.4	4.4	0.57±0.10	0.49	0.20
Ce^{141}			4.0	4.0	0.64	0.35	0.30
Ce^{143}			3.0 ±0.4(3)	3.04	0.61	0.39	0.20
Nd^{147}			1.60±0.04(3)	1.56	0.30	0.20	0.11
Sm^{153}			0.44±0.02(3)	0.45	0.05	0.042	
Eu^{157}			0.038	0.045	0.0165	0.01	

[a] Measured cross section for isotopes.
[b] Cross section corrected for mass chain.
[c] Numbers in parentheses indicate the number of bombardments used to determine the value.
[d] Primary yield measurement.
[e] Includes the subtraction of neutron induced background fission.
[f] The values at energies slightly different from this were normalized to 23.1 Mev (see text).
[g] Normalizations were made similar to (f).

obtained. These cross sections as well as the uncorrected values are tabulated in Table I. When these corrected yields are plotted *versus* mass number, the customary fission yield distribution curves are obtained as shown in Figs. 2 to 8.

At very low energies of this study (<25 Mev), where

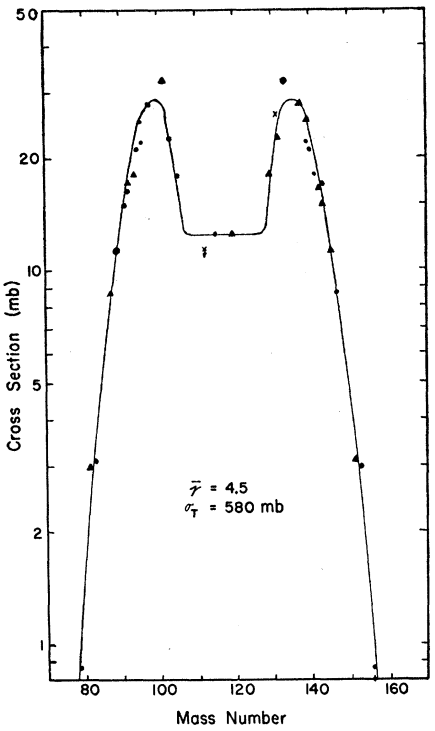

FIG. 4. Fission mass yield curve for 28.7-Mev helium ions. ▲ Reflection points; $\bar{\nu}$ average number of emitted neutrons.

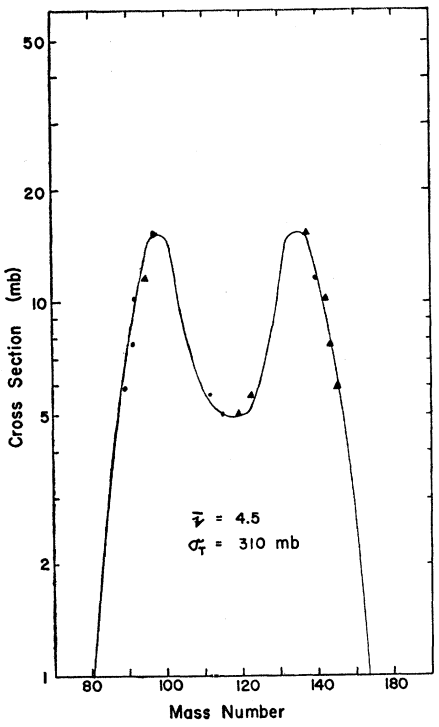

FIG. 5. Fission mass yield curve for 25.9-Mev helium ions. ▲ Reflection points; $\bar{\nu}$ average number of emitted neutrons.

the total cross section and many fission cross sections are changing very rapidly with energy, it became impossible to reproduce exactly the energy of duplicate bombardments. Consequently, a relative method of comparing the results had to be devised. This was done by determining the variation of the cross section of a few of the isotopes with energy and normalizing all other values to a particular energy by use of this curve. Such a curve for $\sigma_{Zr^{97}}$ in the region of 23 Mev is shown in Fig. 9. This is admittedly not a rigorous method but in view of the small energy range over which this method is used, it is believed to be quite reliable.

At ~20 Mev, it becomes very difficult to construct an accurate and detailed fission yield curve with the data collected because of low counting rates, rapid variation of cross sections with energy, and because of the high neutron-induced "background" fission. However, when the ratio of $\sigma_{Zr^{97}}/\sigma_{\text{total}}$ is examined as a function of the excitation energy (E_x) of the compound nucleus, a smooth curve results (Fig. 10). Since the $\sigma_{Zr^{97}}$ values at the lowest energies are believed to be quite reliable, the *total* cross section at 20 Mev can be estimated using this curve to a probable accuracy of ±10–20%. This method of calculating the *total* cross section at the lowest energies is probably as accurate as the mapping of the individual cross sections.

Spallation data were not collected in the present study. However, the percentage of spallation contribution to compound nucleus decay is small except at the lower energies. Spallation yields for U^{235} have been determined by Vandenbosch *et al.*[10] and must be added to the total fission cross sections in order to obtain the cross section for compound nucleus formation (see Table II).

DISCUSSION

A. The Independent Yield Problem

It is beyond the scope of this communication to discuss the problem of independent yields in any detail. Most of the related work has been done at low energies.[35–37] The distribution found at these energies

TABLE II. Total cross sections for U^{235}.

Energy (Mev)	σ_f (mb)	σ_{spall} (mb)	σ_{total} (mb)
39.9	1380	20	1400
33.8	1030	20	1050
28.2	580	20	600
25.9	310	18	328
23.1	87	7	94
20.5	10	1	11

[35] Glendenin, Coryell, and Edwards, *Radio-Chemical Studies: The Fission Products* (McGraw-Hill Book Company, Inc., New York, 1951), National Nuclear Energy Series, Plutonium Project Record, Vol. 9, Div. IV, p. 489.

[36] A. C. Pappas, *Proceedings of the International Conference on the Peaceful Uses of Atomic Energy, Geneva, 1955* (United Nations, New York, 1956), Vol. 7, p. 19. Also Technical Report No. 63, Laboratory of Nuclear Science, Massachusetts Institute of Technology (unpublished).

[37] Many other individual references could be cited but the above two references contain the theoretical ground work for one of the theories regarding the primary yield problem.

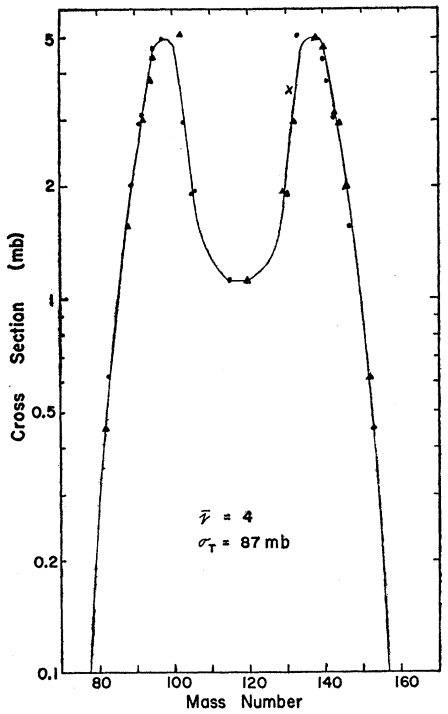

FIG. 6. Fission mass yield curve for 23.1-Mev helium ions. ▲ Reflection points; $\bar{\nu}$ average number of emitted neutrons.

was essentially a Gaussian one. The most probable charge (Z_p) of the distribution corresponding to a given isobar was found not to be in the same n/p ratio as the compound nucleus but instead related to the n/p ratio of the most stable elements near which the fission fragment was formed.

On the other hand, Goeckermann and Perlman[1] performed experiments at 190 Mev which seemed to indicate that the product fission fragments have the same n/p ratios as the parent. More recently, results have been obtained by Alexander and Coryell[38] with 13.6-Mev deuterons on uranium and thorium and by Gibson[11] with intermediate-energy deuterons and alphas on Pu^{239}, Np^{237}, and U^{233}. These two studies are in apparent disagreement with each other, the former data being best explained by the changed charge distribution of Glendenin[35] as modified by Pappas,[36] and the latter by the unchanged charge distribution.

The distribution curve of Gibson is also somewhat broader than that of Glendenin. However, it was found that by making a compromise between the two curves the independent yield correction was, for all nuclides considered, independent (within ±5%) of the type of distribution curve used. The critical part of the estimation of independent yield is in the choice of the proper method of determining the most probable charge (Z_p) and in the determination of the number of neutrons emitted during the entire fission process.

[38] J. M. Alexander and C. D. Coryell, Phys. Rev. **108**, 1274 (1958).

The unchanged charge distribution theory was used to calculate Z_p in the present study, primarily because the experimental yields of I^{133}, Ba^{139}, and Ba^{140} would be much too low if the equal-chain-length postulate were used.

One serious handicap in obtaining a general picture of the primary yield problem is that many of the primary yields which have been measured are located near closed neutron and proton shells. As has already been noticed at low energies,[39] the La^{140} primary yield in this study was also found to be considerably lower (~30%) than expected from the distribution curves. This presumably is due to the emission of an additional

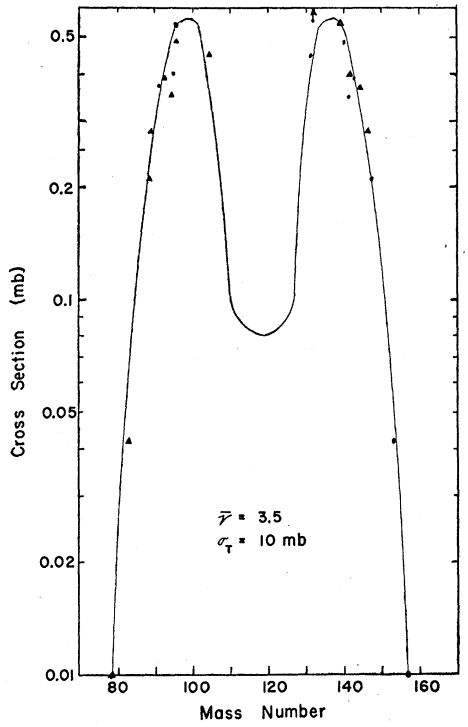

FIG. 7. Fission mass yield curve for 20.5-Mev helium ions. The valley shape has been estimated; for the depth see Figs. 9 and 10. ▲ Reflection points; $\bar{\nu}$ average number of emitted neutrons.

neutron from La^{140} forming La^{139} with a closed neutron shell. Ba^{139} and Ce^{141} yields also frequently appear to be somewhat low and can probably be explained on the same basis. On the other hand, isotopes on the other side of the closed neutron shell (e.g., the iodine isotopes) have relatively larger neutron binding energies causing on the average fewer neutrons to be emitted. There is evidence for this in the fact that the I^{133} yield frequently appears somewhat high when the standard yield correction curve is applied.

Alternatively, the higher calculated yield of I^{133}, especially at lower-energy bombardments, may be due to an admixture of low- and high-energy fission because

[39] W. E. Grumitt and G. M. Milton, J. Inorg. and Nuclear Chem. **5**, 93 (1957).

of fission-spallation competition[40] and consequently the independent yield correction should be based on a most probable Z_p curve determined by a proper weighting of the two postulates (i.e., the changed charge distribution postulate for low-energy fission and the unchanged charge distribution postulate for high-energy fission).

B. Errors and Reproducibility

There are numerous sources of error involved in these determinations. A partial list of possible sources would include such items as counting efficiency, chemical constitution, and reproducibility of the sample, isotopic purity of radioisotopes counted, accuracy of resolving complex decay data, independent yield corrections, standardization of carrier solutions, the use of correct decay schemes and half-lives, uniformity and absolute assay of the target plate, and accurate monitoring of the beam current.

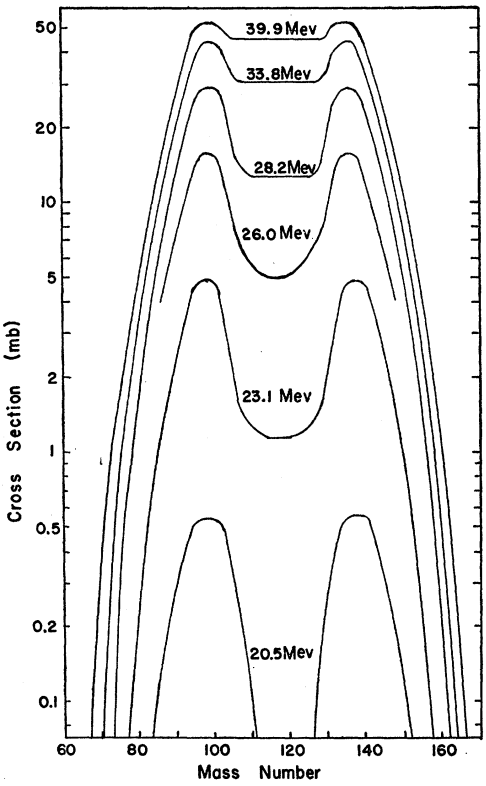

FIG. 8. Composite fission mass yield curves for the various helium ion energies.

After all the cross sections have been determined at a given energy and represented as a mass-yield curve, the total cross section obtained is believed to be accurate to within $\pm 10\%$. The accuracy at 20.5 Mev will be somewhat less than this because of low yields and neutron-induced fission background problems.

[40] A. W. Fairhall, Phys. Rev. **102**, 1335 (1956).

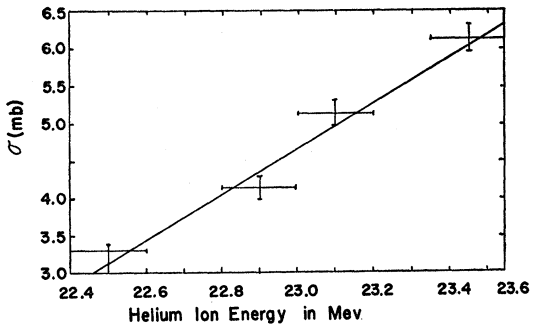

FIG. 9. Variation of the cross section of Zr^{97} with energy in the region of 23-Mev bombarding energies.

C. Neutron Emission

Neutron emission can be inferred by symmetry considerations of the fission yield curve. As has already been mentioned, the average number of neutrons emitted from a fragment appears not to be constant but somewhat dependent on neutron shell closures, more neutrons being emitted from a fragment just beyond a neutron shell closure than from one just before a shell closure. The accuracy of the data does not warrant stating how great this variation is, but it is conceivable that the variation is as large as 0.5 to 1 neutron.

At the highest energy bombardment about 5.5 ± 1.0 neutrons were emitted, while only about 4.0 ± 0.5 neutrons were emitted at the 23-Mev bombardment which seems to be slightly lower than previously reported.[10]

D. Fine Structure

In addition to the variation in the number of neutrons emitted from a fragment, another feature which has shown up quite consistently is the low Ru^{105} yield at the higher energies. This might suggest "triple humped" fission as observed by Fairhall and Jensen[41] and possibly by Turkevich and Niday.[42] The observed phenomenon may be due to experimental error and is a point that will be investigated in further detail.

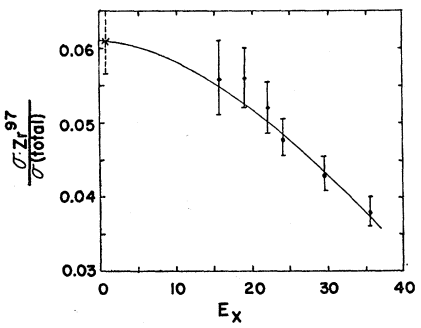

FIG. 10. The variation of $\sigma_{Zr^{97}}/\sigma_{\text{total}}$ with bombarding energy.

[41] A. W. Fairhall and R. C. Jensen, Phys. Rev. **109**, 942 (1958).
[42] A. Turkevich and J. B. Niday, Phys. Rev. **84**, 52 (1951).

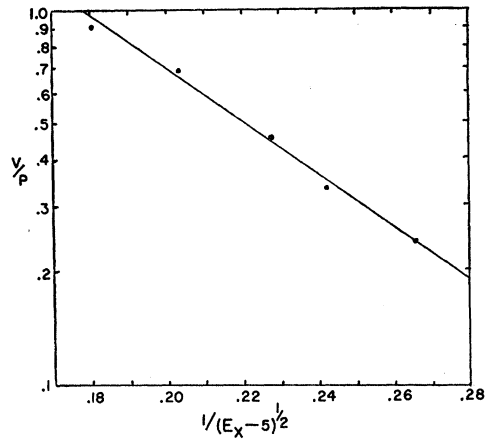

FIG. 11. The relationship of the valley to peak ratio to the excitation energy of the compound nucleus.

E. Valley to Peak Ratio

It has been shown in some models of fission that the valley to peak ratio should be related to the excitation energy of the compound nucleus. Good agreement is obtained when the v/p *versus* $1/(E_x-5)^{\frac{1}{2}}$ function suggested by Fowler, Jones, and Phaeler[43,44] is used as is shown in Fig. 11. Several attempts have been made to correlate all known valley to peak ratios[11,17,45] but will not be given here largely because so much of the reported data are not of sufficient accuracy to warrant it. Further, it is likely that the treatment is oversimplified.[45] Studies are presently underway in our laboratory to take into consideration other parameters such as the bombarding particle, the Z^2/A of the compound nucleus and its quadrupole moment, and degree of de-excitation of the compound nucleus caused by particle emission prior to fission.

F. Radius Calculations

When the fission and spallation contributions to compound nucleus cross section are added, the total cross section appears as is shown in Fig. 12. Blatt and Weisskopf[46] and Shapiro[47] have calculated theoretical values for compound nucleus interaction assuming that the nucleus has a well-defined spherical surface of radius R. The curves produced from these tabulated values are also shown in Fig. 12 for the radius parameters (r_0) of 1.3×10^{-13} cm and 1.5×10^{-13} cm, where r_0 is related to the radius by

$$R=r_0A^{\frac{1}{3}}.$$

The agreement with theory is dependent on the range-energy curve used in determining the bombardment energy and the initial cyclotron beam energy. The difference in energy is nearly 1 Mev for 40-Mev helium ions depending on whether the theoretical range-energy curves of Aron, Hoffman, and Williams[23] or the data of Bichsel, Mozley, and Aron[22] are used. Since the range-energy relationships for protons were experimentally determined by the latter, from which helium-ion ranges can be inferred, it is believed that these new ranges are an improvement over the older theoretical ones. A considerable improvement in fit is also noted in the data presented here as is shown in Fig. 12.

The new range-energy relationships make suspect the bombarding energies of much of the previous work, especially for results obtained for bombarding energies below the nuclear potential barrier where cross sections are very sensitive to energy. No attempt has been made as yet to recalculate previous data but it can be stated that the new range curves would decrease the energy values obtained when the Aron, Hoffman, and Williams curves are used.

SUMMARY

1. The fission yield of U^{235} induced by 20- to 40-Mev helium ions is asymmetric with the symmetric mode increasing rapidly throughout the range. There is some indication that there may be some "peaking" at mass 115 corresponding to symmetric fission but there is no evidence of the onset of predominantly symmetric fission below 40 Mev.

2. The experimental cross section data obtained in this study correspond to compound nucleus theory

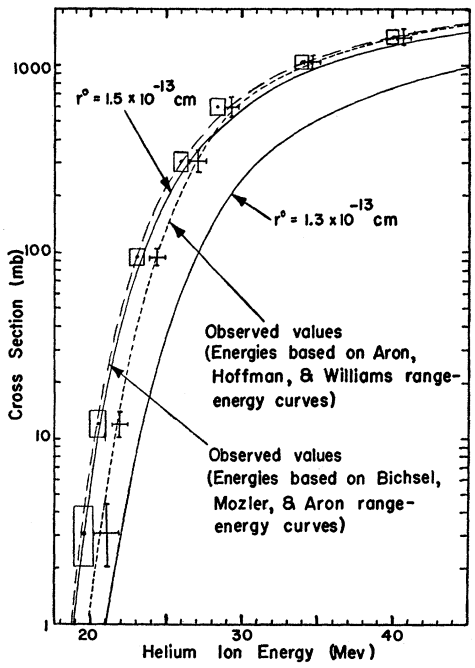

FIG. 12. Total cross sections for compound nucleus formation *versus* bombarding energy and a comparison with compound nucleus theory.

[43] Jones, Fowler, and Phaeler, Phys. Rev. **87**, 174 (1952).
[44] Fowler, Jones, and Phaeler, Phys. Rev. **88**, 71 (1952).
[45] Jones, Trimmick, Phaeler, and Handley, Phys. Rev. **99**, 184 (1955).
[46] J. M. Blatt and V. F. Weisskopf, *Theoretical Nuclear Physics* (John Wiley & Sons, Inc., New York, 1952).
[47] M. M. Shapiro, Phys. Rev. **90**, 171 (1953).

using a radius parameter of $r_0=1.5\times10^{-13}$ cm when recent experimentally obtained range-energy curves[22] are used for the basis of determining the bombardment energies.

3. As previously observed, the valley to peak ratio can be related to the excitation energy of the compound nucleus.

4. A smaller number of neutrons emitted per fission is found than previously reported.

ACKNOWLEDGMENTS

The authors wish to acknowledge the assistance and helpful discussions of R. D. Griffioen, L. J. Colby, Jr., and M. J. LaSalle. The cooperation of W. Ramler, A. Schulke, and the crew of the Argonne National Laboratory cyclotron is also very greatly appreciated.

APPENDIX

The chemistry scheme was devised so that nearly all of the radioelements needed for the mass-yield curve could be isolated successively from one target solution. Publications, compilations, and works by Meinke,[48] Duval,[49] Howell and Furman,[50] and many others proved to be helpful in providing chemistry procedures and precipitates suitable for this study.

A flow diagram of the general chemistry separation scheme is shown in Fig. 13. The following is a summary of the chemical separation method and isotope identification for each element investigated.

Zinc-Gallium

KSCN-$HgCl_2$ reagent[50] was used to precipitate $ZnHg(SCN)_4$ from solution. The precipitate was dissolved in conc. HNO_3· NH_4Cl and Ga(III) carrier were added to the solution and NH_4OH added to precipitate the $Ga(OH)_3$. The time of this separation was noted so that the amount of Ga^{72} grown in at the time of the final separation could be determined. The Zn was next precipitated with $(NH_4)_2HPO_4$, dissolved in dilute HCl and precipitated again as $ZnHg(SCN)_4$. It was then dried and weighed to determine the chemical yield of Zn. The precipitate was dissolved in HNO_3. NH_4Cl and 5 mg of Ga(III) carrier was added and the solution was allowed to stand until the Ga^{72} activity had grown in. $Ga(OH)_3$ was then precipitated, dissolved in 6*N* HCl, extracted in ether, and extracted back into H_2O. $Ga(OH)_3$ was again precipitated, mounted, dried at >410°C,[49] weighed, and counted for Ga^{72} activity.

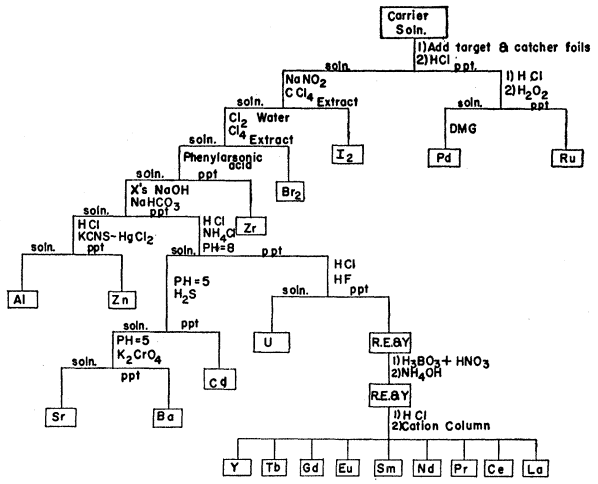

FIG. 13. General chemistry separation scheme.

Bromine

Small portions of chlorine water were used to oxidize the bromide in solution to free bromine, which was then extracted with CCl_4. (CCl_4 frequently contains impurities with unsaturated linkages. Passing Cl_2 gas into the CCl_4 followed by NaOH washings to remove excess Cl_2 saturates these impurities so that they do not react with the Br_2.) The Br_2 was extracted back into water containing HSO_3^-. The solution was then scavenged for iodine. H_2SO_4 followed by the dropwise addition of 0.1*M* $KMnO_4$ was used to oxidize the Br^- which was then extracted first into CCl_4 and then back into water containing HSO_3^-. After the solution was boiled to remove excess HSO_3^-, $AgNO_3$ was added to precipitate AgBr which was then mounted, dried at 110°C, weighed, and counted for Br^{83} activity. Special consideration was made in the final calculations for delay in the onset of the Br^{83} activity because of the Se^{83m} (25-min) state preceding it in the decay chain.[34]

Strontium

Strontium and barium were precipitated as the carbonates and dissolved in HCl. The barium separation and scavenging was made by the standard chromate precipitation method[48] after which the strontium was precipitated from a neutral solution as the oxalate. The precipitate was washed, mounted, dried at 200°C, weighed as SrC_2O_4,[49] and counted for Sr^{89}, Sr^{91}, Sr^{92}, Y^{91}, and Y^{92} activities, the latter two growing in after the strontium rare earth separation was made.

Zirconium

Phenylarsonic acid was used to precipitate Zr(IV) from solution. This precipitate was converted to $Zr(OH)_4$ by the addition of conc. NaOH. The precipitate was then dissolved in 6*M* HCl and Zr(IV) finally precipitated as the mandelate.[51] The precipitate was washed, dried at 110°C, weighed as $Zr(C_6H_5CHOHCO_2)_4$,[49] and counted for Zr^{97}-Nb^{97} and for Zr^{95}-Nb^{95} activities.

[48] W. W. Meinke, Atomic Energy Commission Report AECD-2738, 1949 (unpublished).

[49] C. L. Duval, *Inorganic Thermogravimetric Analysis* (Elsevier Publishing Company, New York, 1953).

[50] *Scott's Standard Methods of Chemical Analysis*, edited by N. Howell and N. H. Furman (D. Van Nostrand Company, Inc., New York, 1939), fifth edition.

[51] C. A. Kumins, Anal. Chem. **19**, 376 (1947).

Ruthenium[48]

Metallic Ru^0 was precipitated from the solution during the dissolution of the target. Care was taken that Ru(III) carrier was present during the entire dissolution and additional amounts of aluminum added to reduce the Ru(III) left in solution after the dissolution of the target was complete. The metallic ruthenium was dissolved in a basic KClO solution and transferred to a ruthenium distillation flask. The addition of $NaBiO_3$ and a H_3PO_4-$HClO_4$ mixture produced RuO_4 which was distllled from the solution by gentle heating and was collected in 6*N* NaOH. $RuO_2 \cdot xH_2O$ formed when 95% EtOH was added and the solution heated to ~85°C. The precipitate was immediately dissolved in HCl and the ruthenium was reduced to the metal with aluminum. The metallic ruthenium was dried in a small test tube, weighed, and counted in a calibrated NaI(Tl) well-type scintillation counter for Ru^{103} and Ru^{105} activities.

Palladium

Palladium was reduced in the solution in the same way as was ruthenium. Pd^0 is oxidized by 30% H_2O_2, separating it from the metallic ruthenium. Pd(II) was then precipitated using dimethylglyoxime (DMG) which was again dissolved in conc. HNO_3. The solution was scavenged for silver, and the PdDMG again precipitated, in which form it was dried and weighed for yield determination. The precipitate was then dissolved, Ag carrier added, and the solution allowed to stand until Ag^{112} activity had grown into secular equilibrium.

AgI was then precipitated from the solution, mounted, dried at 110°C, weighed, and counted for the Ag^{112} activity. Calculations necessitate an accurate knowledge of the time of the final Pd-Ag separation.

Cadmium

$Cd(OH)_2$ was precipitated from a strongly basic solution along with Sr, Ba, Y, and the rare earths. The precipitates were treated with HCl and after the separation of the rare earths (and Y), H_2S was passed into the solution precipitating CdS. The precipitate was dissolved in HCl and the resultant solution scavenged with antimony by precipitating it as the sulfide from a 2*M* HCl solution. CdS was reprecipitated at pH=5, dissolved in conc. HCl, placed on a column bed containing Dowex 1-X[8] anion resin, and eluted with 0.75*M* H_2SO_4. CdS was precipitated from the fractions collected and redissolved in conc. HCl. The H_2S was removed by boiling and Cd was finally precipitated as $Cd(NH_4)PO_4 \cdot H_2O$. It was then dried at 110°C, weighed, and counted for Cd^{115} and Cd^{115m} activities.

Iodine

$NaNO_2$ was added to the solution oxidizing the iodide to free iodine which was first extracted into CCl_4 and then back into water contains HSO_3^-. The cycle was again repeated, the solution boiled to remove excess HSO_3^-, and $AgNO_3$ added to precipitate AgI. The precipitate was placed in a small test tube, dried at 110°C, weighed, and counted in the calibrated NaI(Tl) crystal scintillation counter. Activities due to I^{133} and I^{131} (and their daughters) were followed, from which cross section calculations were made.

Barium

Barium follows strontium in the chemical procedure and was separated from it with K_2CrO_4. The $BaCrO_4$ was dissolved in conc. HCl to which an equal volume of Et_2O was added. The mixture was cooled in an ice-brine bath and HCl gas passed through the solution, precipitating $BaCl_2 \cdot 2H_2O$. The precipitate was dissolved in water and $BaCrO_4$ reprecipitated. This was then washed, mounted, dried at 110°C, weighed, and counted for Ba^{139} and Ba^{140}-La^{140} activities.

Rare Earths and Yttrium

These elements were separated from the solution as the hydroxides, dissolved in HCl, and then precipitated as the fluorides with HF. These precipitates were dissolved in a HNO_3-H_3BO_3 mixture from which the hydroxides were again precipitated. Upon dissolution in dilute HCl, the rare earths and yttrium were placed on a cation exchange column and eluted with a varying pH lactic acid eluent.[52] The addition of $(NH_4)_2C_2O_4$ to the fractions collected precipitated the elements as the oxalates which were dried under a vacuum and then mounted, weighed, and counted. The following were the isotopes counted: Y^{93}, La^{140} (for independent yield measurements), Ce^{141} and Ce^{143} in the scintillation counter, Pr^{143}, Pr^{145}, Nd^{147}, Sm^{153}, Eu^{156}, Eu^{157}, Gd^{159}, and Tb^{161}.

[52] W. E. Nervik, J. Phys. Chem. **59**, 690 (1955).